

## 5.1 LARGE-AMPLITUDE GRAVITY-WAVE BREAKING OVER THE GREENLAND LEE AND THE SUBSEQUENT FORMATION OF DOWNSTREAM SYNOPTIC-SCALE TROPOPAUSE FOLDING AND STRATOSPHERIC-TROPOSPHERIC EXCHANGE

Melvyn A. Shapiro<sup>1</sup>, Simon Low-Nam<sup>2</sup>, Haraldur Olafsson<sup>3</sup>, James Doyle<sup>4</sup> and Piotr K. Smolarkiewicz<sup>2</sup>

<sup>1</sup>NOAA/Environmental Technology Laboratory, Boulder, CO

<sup>2</sup>National Center for Atmospheric Research, Boulder, CO

<sup>3</sup>University of Iceland, Icelandic Meteorological Office, Reykjavik, Iceland

<sup>4</sup>Naval Research Laboratory, Monterey, CA

### 1. INTRODUCTION

The importance of mountain waves for numerical weather prediction is underscored by the numerous studies that document their impact on the atmospheric momentum balance (e.g., Eliassen and Palm 1961), turbulence generation (e.g., Lilly 1978), and the creation of severe downslope winds (e.g., Smith 1985). Large-amplitude internal gravity waves may be generated as a consequence of stably stratified air that is forced to rise over topography. Amplification of upward-propagating gravity waves occurs, in part, due to the decrease in atmospheric density with height and may result in subsequent wave overturning and turbulent breakdown (e.g., Bacmeister and Schoeberl 1988).

The present extended abstract describes an extreme topographic flow event that occurred in the eastern lee of Greenland. Observed surface winds over the Greenland Sea and Iceland exceeded  $40 \text{ m s}^{-1}$  as rapid synoptic-scale cyclone development ensued in the east- Greenland coastal zone. The lee cyclone developed at the rate of 37 mb in 18 h. Figure 1 shows the NOAA/polar satellite IR image at the height of the storm development. The event included the formation of a  $\sim 75 \text{ ms}^{-1}$  tropopause-based jet stream at 7-km altitude. The upper jet and associated tropopause fold extended northeastward from the Greenland to west of Iceland. Olafsson (1998) has shown that the synoptic development around Iceland can be very sensitive

to how numerical models represent Greenland (see also Olafsson and Shapiro 2002, this volume).

The severity of this event warranted its simulation and diagnosis with the NCAR/Penn State MM5 multi-scale prediction system. Results of the simulation show massive gravity-wave breaking, extending  $\sim 500 \text{ km}$  along the southeast coast of Greenland. The associated hydraulic jump at the wave trough extended from 2 km to above 7 km, as the isentropic surfaces ascended near adiabatically in association within the jump. Upward wave propagation resulted in comparable wave breaking aloft in the layer 10-20 km. The extreme depth of the lower-tropospheric adiabatic cooling associated with the hydraulic jump gave rise to a  $\sim 500 \text{ km}$  diameter 10C cold pool in the layer 2-6 km. The cold pool expanded  $\sim 1000 \text{ km}$  eastward across the Greenland Sea, with strong upper-level frontal/jet stream formation, tropopause folding and potential vorticity (PV) banner development downstream from the region of wave breaking. Trajectory analysis suggests that ozone was extruded from the arctic lower stratosphere and transported into the lower troposphere during this event. The realism of the simulation is supported by: i) QUIKSCAT scatterometer satellite surface wind measurements over the Greenland and Norwegian Sea; ii) Satellite multi-pectral observations of polar-stratospheric clouds over Greenland at  $\sim 20 \text{ km}$  derived from sun-shadow trigonometry.

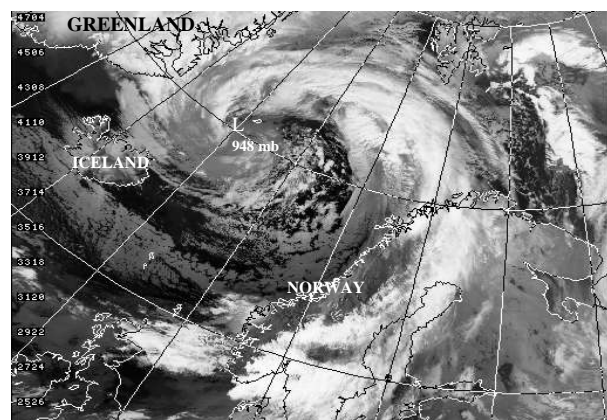


**Fig. 1.** NOAA polar satellite IR image of the Greenland lee cyclone at 1200 UTC 10 Nov. 2001 (Dundee satellite Receiving Station).

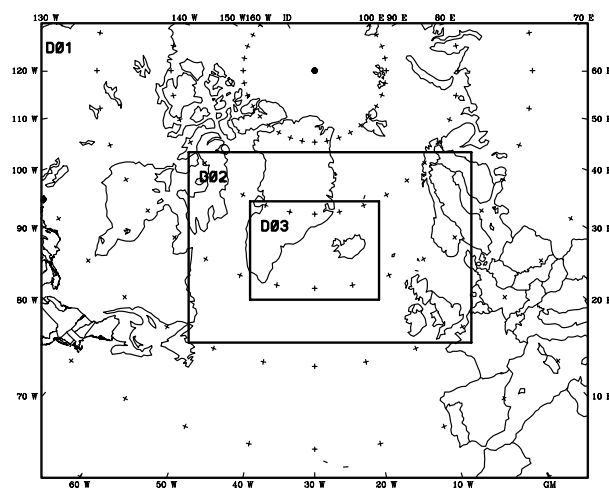


**Fig. 2.** MM5 two-way interactive triple mesh with resolutions of 90 (outer); 30 (middle); 10 km (inner).

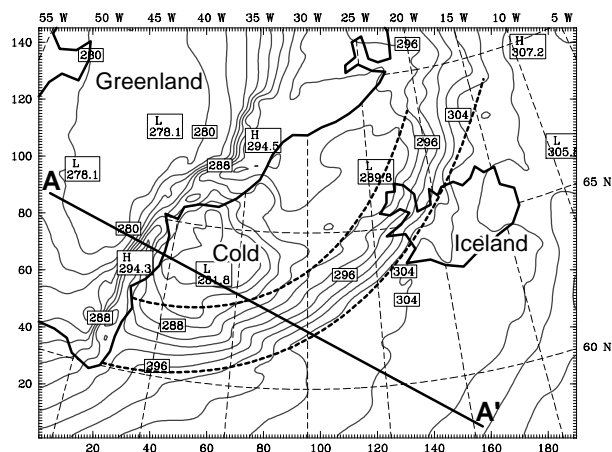


**Fig. 3.** 4-km potential temperature (2-K intervals) at 0000 UTC 10 Nov. 2001: frontal boundaries, dashed; projection AA' for Figs. 6, 7, and 8.

etry and infrared cloud-top temperatures; and iii) conventional observations.

## 2. THE NUMERICAL SIMULATION

Figure 2 presents the triple mesh domains for the NCAR/Penn State MM5 numerical model simulation of this event. This simulation was performed as a two-way, interactive, triple-mesh, with horizontal resolutions of 90, 30, and 10 km, and with 62 levels. This Section opens with a discussion of the synoptic-scale aspects of the situation (Section 2.1), followed by the description of the attendant topographic wave breaking (Section 2.2) and downstream tropopause folding (Section 2.3).

### 2.1 The Synoptic-scale Perspective

Figure 3 shows the 24-h simulation of 4-km potential temperature field at 0000 UTC 10 Nov. 2001. Key features in this analysis include: i) the -12 K mid-tropospheric frontal zone extending from the southern tip of Greenland to north of Iceland, ii) the pool of cold air extending northeastward from the southeastern tip of Greenland to the north of Iceland, and iii) the sharp thermal gradient over the east Greenland lee indicative of the region of topographic wave breaking discussed below. The companion 7-km potential vorticity and velocity vectors (Fig. 4.) shows a substantial PV banner and  $>60 \text{ ms}^{-1}$  jet stream extending northeastward from the east coast of Greenland. This synoptic-scale PV anomaly exceeds 8 PVU, and was much weaker in a numerical simulation (not shown) in which the Greenland topography was removed. The substantial cyclonic PV advection along the east Greenland coast, northwest of Iceland, was vertically aligned with the rapidly developing surface cyclone, visualized in its mature phase (12 h later) in the Fig.1 satellite image.

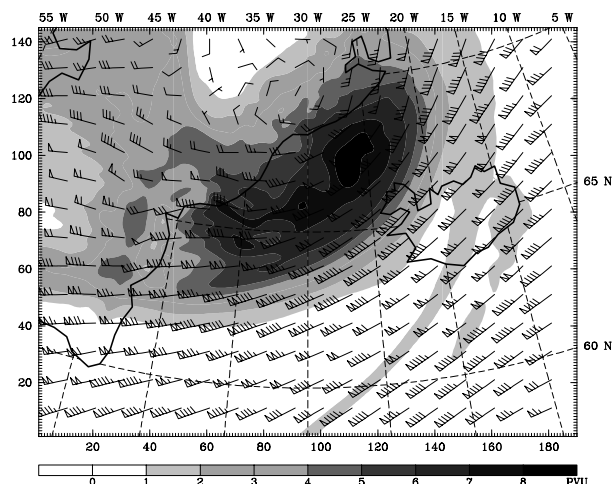


**Fig. 4.** Potential vorticity (PVU, shaded) at 0000 UTC 10 Nov. 2001 and velocity vectors (flag =  $25 \text{ ms}^{-1}$ ).

### 2.2 Topographic-Wave Breaking

The current limit in knowledge of gravity wave breaking can be attributed, in part, to lack of observations. During the Fronts and Atlantic Storm-Track Experiment (FASTEX), a large-amplitude gravity wave was observed in the Greenland lee on 29 January 1997. Dropsonde observations by the NOAA/G-4 aircraft presented the opportunity to study this example of topographically forced gravity-waves and to assess the ability of high-resolution numerical models to predict such phenomena. Figure 5

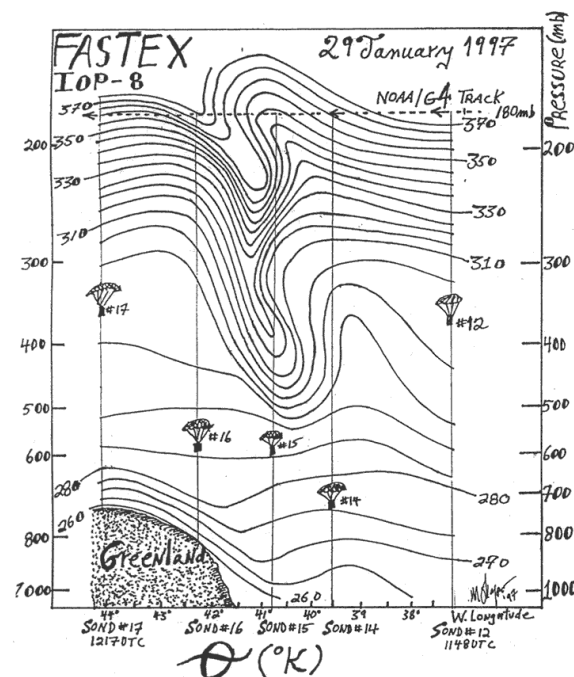


**Fig. 5.** Cross section of potential temperature (K) at ~1200 UTC 29 January 1997 derived from dropsondes (numbered 12-17) from the NOAA/G-4 aircraft.

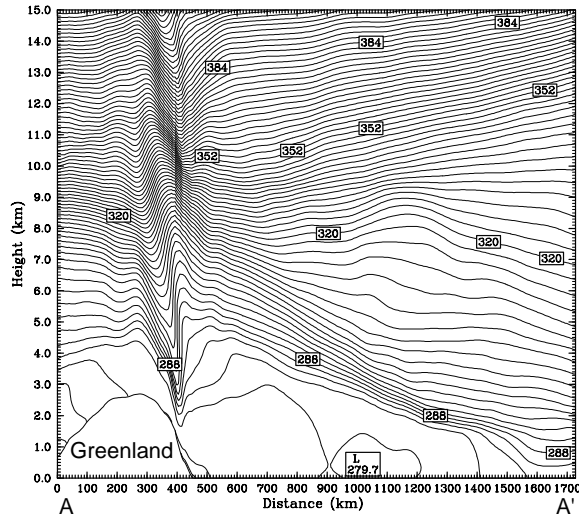


**Fig. 6.** Cross section of potential temperature (K) at 0000 UTC 10 November 2001, along the line AA' of Fig. 3.

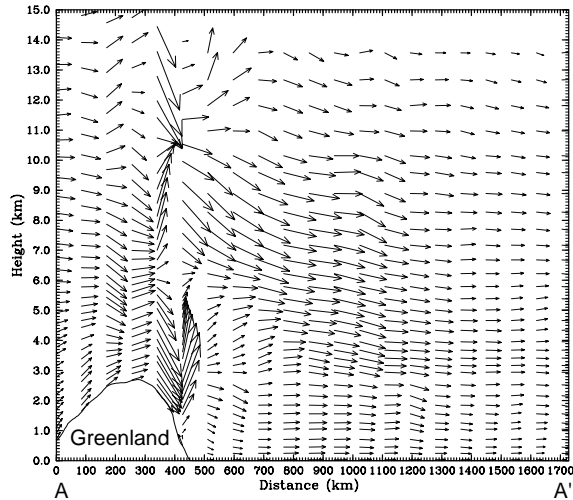


**Fig. 7.** Two-dimensional (x,z) velocity vector for Fig. 6. Maximum horizontal and vertical wind components ( $u, w$ ) are 45 and 2  $\text{ms}^{-1}$ , respectively

presents the analysis of the FASTEX gravity wave simulated by Doyle et al. (1998a,b) for comparison with the uncorroborated wave breaking simulation in the present study.

The MM5 24-h simulation of the vertical structure of the Greenland-lee gravity wave and downstream tropopause fold at 0000 UTC 10 Nov. 2001 is shown in the cross-sections of: i) potential temperature (Fig. 6), ii) along-section velocity vector (Fig. 7), and iii) horizontal wind speed and PV (Fig. 8). The potential temperature distribution (Fig. 6, along the projection line AA' of Fig. 2) reveals major upward-propagating gravity waves above the lee escarpment of Greenland, with two westward tilted wave in the layers 2-10 and 10-15+ km. Note the near-adiabatic rise of the isentropes from 2 to ~7 km associated with the

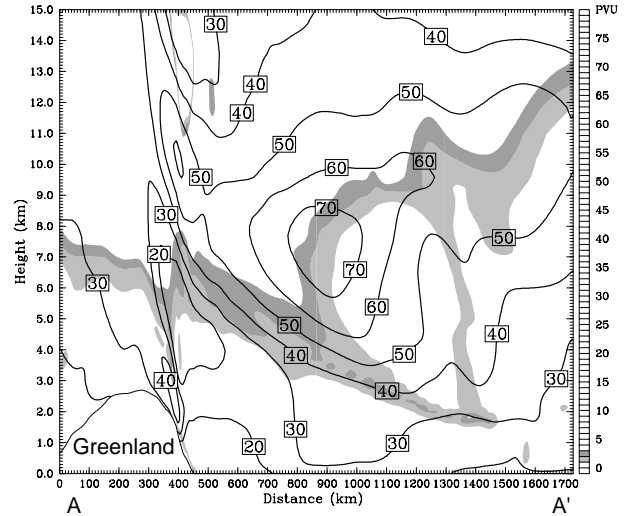


**Fig. 8.** Cross section of horizontal wind velocity ( $\text{ms}^{-1}$ ) and PV (2-6 PVU, shaded) for Fig. 6.

the hydraulic jump east of the wave trough axis. Comparing the FASTEX observed Greenland lee wave of 29 January 1997 (Fig. 5) with the 10 November 2001 event (Fig. 6) shows a notable similarity between the previously observed and the recently simulated event, respectively.

The vertical circulation in the plane of the cross section (Fig. 7) shows the deformation of the cross-Greenland flow in the regions of wave amplification and breaking. Maximum vertical velocities were  $\sim 2 \text{ ms}^{-1}$  where the horizontal flow normal to the wave front decelerated. The cross section of horizontal wind speed (Fig. 8) shows a  $> 40 \text{ ms}^{-1}$  near-surface speed maximum on the eastern slope of Greenland situated just beneath the minimum downward extent of the wave trough in Fig. 6. A second localized maxima is found within the highly stratified sloping layer between 9 and 15 km in association with wave propagation into the upper stratosphere. The potential temperature, horizontal and vertical wind flows simulated for this event (Figs. 6, 7, and 8) are representative of earlier studies of observed and idealized stably stratified flows in the vicinity of steep topography, such as those cited in the introduction to this abstract.

### 2.3 Tropopause Folding

We next draw attention to the dramatic PV-tropopause fold and  $\sim 7\text{-km}$ ,  $> 75 \text{ ms}^{-1}$  jet stream in Fig. 8, and associated frontal zone (Figs. 3 and 6). This tropopause fold and upper-level jet stream/frontal-zone system formed downstream from the Greenland gravity wave described above. The PV analysis (Fig. 8) shows the downward intrusion of stratospheric values of PV in excess of 2 PVU, consistent with diagnosed air-parcel trajectories (not shown) that had originated from  $\sim 8 \text{ km}$  in the arctic stratosphere upstream of Greenland and penetrated to below 2 km over the northwest coast of Iceland. Tropopause folding and



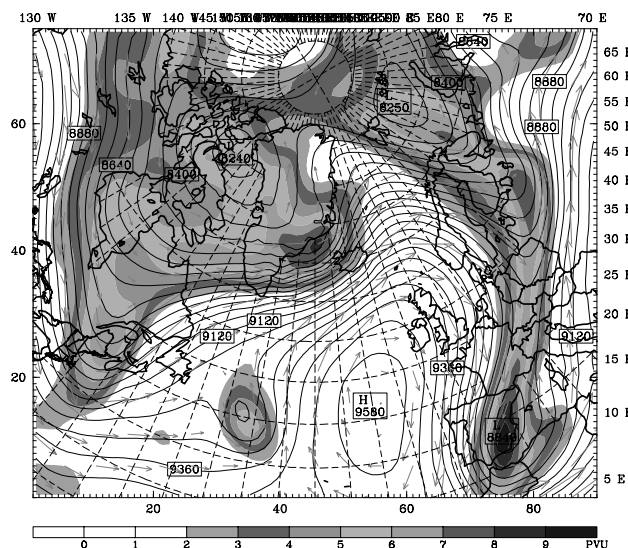


**Fig. 9.** 24-h simulation of potential vorticity (PVU, shaded) and 300-mb geopotential (m, thin lines) at 0000 UTC 10 Nov. 2001.

exchange of air from the stratosphere into the troposphere was evident in vertical sections across the entirety of the upper front (Fig. 3) and PV anomaly (Fig. 4).

### 3. THE MULTI-SCALE PERSPECTIVE

It is of interest to consider the mesoscale through planetary-scale influence of Greenland on extratropical life cycles. Figure 9 presents the 24-h simulation of 300-mb PV and geopotential for the outer domain of Fig. 2. A comparison between this simulation and one without Greenland topography (not shown) reveals that the synoptic-scale trough and positive PV anomaly in the eastern lee of Greenland (Fig. 9 and 3) was much weaker in the zero Greenland topography experiment. Greenland lee cyclogenesis did not occur without inclusion of the Greenland topography.

There is evidence of the impact of Greenland on downstream Rossby wave dispersion. The downstream PV filament extending from north of Scandinavia to Spain (Fig. 9) and subsequent cyclogenesis over the Mediterranean Sea differed substantially between the two simulations. The apparent influence of localized topography on Rossby wave initiation and dispersion has been addressed by, e.g., Grose and Hoskins (1979), and Smolarkiewicz et al. (2001), and further illustrated in Fig. 10.

### 4. CONCLUSION

In conclusion, this study suggests that Greenland modulates the full spectrum of atmospheric motion. This includes the interplay between topographically forced vertically propagating gravity waves, horizontally dispersive topographic Rossby waves, and transient and dispersive Rossby waves in the westerlies. Future research

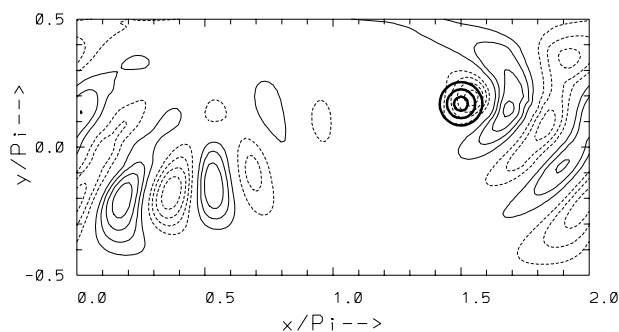


**Fig. 10.** Idealized simulation of planetary-wave propagation on a sphere excited by large-scale topography, c.f., Smolarkiewicz, et al. (2001). Meridional wind ( $\text{ms}^{-1}$ , negative; dashed). Mountain, solid circles (maximum height of 2 km).

will address the influence of gravity-wave breaking in the Greenland lee on the predictability of scales spanning the mesoscale through planetary-scale of motion.

### ACKNOWLEDGEMENTS

The first author's research was partially supported by ONR grant 0602435N and the NASA/Office of Earth Science.

### 5. REFERENCES

- Bacmeister, J.T., and M.R. Schoeberl, 1988: Break-down of vertically propagating two-dimensional gravity waves forced by orography. *J. Atmos. Sci.*, **46**, 2109-2134.
- Doyle, J. D., M. Shapiro, D. Bartels, and R. Gall, 1998a: The numerical simulation of a breaking gravity wave during FASTEX. *Research Activities in Atmospheric and Oceanic Modeling*, WMO Commission for Atmospheric Sciences, 5.19-5.20.
- Doyle, J. D., M. Shapiro, D. Bartels, and R. Gall, 1998b: The numerical simulation and validation of a breaking gravity wave during FASTEX. *Sixteenth Conference on Weather Analysis and Forecasting*, 11-16 Jan. 1998, Phoenix, AZ, 460-462.
- Eliassen, A., and E. Palm 1961: On the transfer of energy in stationary mountain waves. *Geophys. Publ.*, **22**, 1-23.
- Grose, W. L., and B. J. Hoskins, 1979: On the influence of orography on large-scale atmospheric flow. *J. Atmos. Sci.*, **36**, 223-234.
- Lilly, D. K., 1978: A severe downslope windstorm and aircraft turbulence event induced by a mountain wave. *J. Atmos. Sci.*, **35**, 59-77.
- Olafsson, H., 1998: Different prediction by two NWP models of the surface pressure field east of Iceland. *Meteorol. Apps.*, **5**, 253-261.
- Olafsson, H. and M. A. Shapiro, 2002: Observations and numerical simulations of a wake and a tip jet in an orographically generated strong windstorm over Iceland, *10th Conf. on Mountain Meteorology*, Salt Lake City, Utah.
- Smith, R. B., 1985: On severe downslope winds. *J. Atmos. Sci.*, **43**, 2597-2603.
- Smolarkiewicz, P. K., L. Margolin, and A. Wyszogrodzki, 2001: A class of nonhydrostatic models. *J. Atmos. Sci.*, **58**, 349-364.